Earth pressure on a vertical shaft considering the arching effect in c-ϕ soil

In-Mo Lee [1], Do-Hoon Kim [2], Kyoung-Yul Kim [3] and Seok-Won Lee [*4]

[1] *School of Civil, Environmental, and Architectural Engineering, Korea University, Seoul, Korea*
[2] *Hyundai Eng. and Construction Co., Ltd., Seoul, Korea (former Ph.D. Student in Korea University)*
[3] *Korea Electric Power Research Institute, Deajeon, Korea*
[4] *Department of Civil and Environmental System Engineering, Konkuk University, Seoul, Korea*

Abstract. A new earth pressure equation considering the arching effect in c-ϕ soils was proposed for the accurate calculation of earth pressure on circular vertical shafts. The arching effect and the subsequent load recovery phenomenon occurring due to multi-step excavation were quantitatively investigated through laboratory tests. The new earth pressure equation was verified by comparing the test results with the earth pressures predicted by new equation in various soil conditions. Resulting from testing by using multi-step excavation, the arching effect and load recovery were clearly observed. The test results in c-ϕ soil showed that even a small amount of cohesion can cause the earth pressure to decrease significantly. Therefore, predicting earth pressure without considering such cohesion can lead to overestimation of earth pressure. The test results in various ground conditions demonstrated that the newly proposed equation, which enables consideration of cohesion as appropriate, is the most reliable equation for predicting earth pressure in both ϕ soil and c-ϕ soil. The comparison of the theoretical equations with the field data measured on a real construction site also highlighted the best-fitness of the theoretical equation in predicting earth pressure.

1. Introduction

When excavating the circular vertical shaft into the ground, a smaller earth pressure is induced on the shaft wall than in the 2-dimensional plane strain condition due to the 3-dimensional arching effect. Theoretical studies on earth pressure considering the arching effect on the circular vertical shaft have been carried out by many researchers. A calculation method of earth pressure has been suggested by various researchers: Terzaghi (1943) employed a theory of circular opening, Prater (1977), Wong and Kaiser (1988), and Shin (2004) used a limit equilibrium analysis method, and Cheng *et al.* (2007), Liu and Wang (2008) and Liu *et al.* (2009) employed a slip line method. Lee *et al.* (2007) carried out a study on the calculation method of earth pressure in multi-layered soil. Zheng *et al.* (2015) employed a lower-bound theorem of limit analysis combined with Rankine's earth pressure theory and the Mohr-Coulomb yield criterion. In addition, a calculation method of

---

*Corresponding author, Professor, E-mail: swlee@konkuk.ac.kr

seismic earth pressure has been suggested by various researchers (Shukla *et al*. 2009, Iskander *et al*. 2013, Nian *et al*. 2014, Ismeik and Shaqour 2015). However, as these studies presupposed cohesionless ($c = 0$) ϕ soil, or c soil with $\phi = 0$, it is difficult to apply them to c-ϕ soils that have both cohesion (c) and friction (ϕ). Experimental studies on the 3-dimensional earth pressure due to shaft excavation have been carried out by many researchers. By using the centrifuge model test (Imamura *et al*. 1999) and the soil chamber test (Fujii *et al*. 1994, Herten and Pulsfort 1999, Shin 2004, Lee *et al*. 2007, Moradi and Abbasnejad 2015), the various cross sections of the shaft as well as the various directions of deformation were examined. However, three drawbacks were revealed as follows. Firstly, in all previous tests, only the shaft excavated in one step (single-step excavation) was simulated, which cannot reflect the load recovery. Secondly, all previous tests were conducted only with cohesionless ($c = 0$) ϕ soil. Lastly, no consideration was taken of the shape ratio ($n = H/R$ = Height/Radius) of the shaft.

In this study, firstly a formulation for calculating the active earth pressure on a circular vertical shaft in c-ϕ soils, considering the arching effect of the ground was proposed (Kim 2011). To check the applicability of the proposed earth pressure equation, the earth pressure was calculated by using the new equation under diverse soil conditions, and the result was compared with those of formerly suggested earth pressure equations (e.g., Rankine's earth pressure). Secondly, a large-scale soil chamber which can change the shape ratio and can simulate the multi-step excavation was manufactured. By conducting the single-step excavation tests, the characteristics of earth pressure distribution according to the shape ratio were studied. Distributions of earth pressure acting on the shaft wall under multi-step excavation in both cohesionless ϕ soil and cohesive c-ϕ soil were tested to investigate the influence of the arching effect and the cohesion. The earth pressure in the multi-layered ground was examined. Lastly, the laboratory test result and the actual field measurement data were compared with the result of the new earth pressure equation (Kim 2011) in order to verify the validity of the new equation.

2. Earth pressure equation in *c-* *φ* soils

Kim (2011) derived a new active earth pressure equation applicable to the c-ϕ soils as Eq. (1). Here, the coefficient of tangential earth pressure (λ) was assumed as '$1 - \sin \phi$' and the shape of the failure zone was set as conical with a '$45° + \phi / 2$' failure surface slope (β).

$$p_i = k_{wa} \times \sigma_v \tag{1}$$

Where: $\sigma_v = \left(q - \dfrac{T}{S} \right) e^{-Sz} + \dfrac{T}{S}$

$$T = \gamma - \frac{2\pi}{A} \left\{ c_w R + c(r + R) \left(1 + \frac{1 + \tan \beta \tan \phi}{\tan \beta - \tan \phi} \right) \right\}$$

$$S = \frac{2\pi}{A} \left\{ k_{wa} R \tan \delta + (k_{wa} R + \lambda r) \frac{1 + \tan \beta \tan \phi}{\tan \beta - \tan \phi} \right\}$$

$$k_{wa} = \frac{3(K_i \cos^2 \theta + \sin^2 \theta)}{3K_i - (K_i - 1)\cos^2 \theta}$$

$$K_i = \frac{\sigma_1}{\sigma_3} = \frac{1}{\tan^2\left(45 - \frac{\phi}{2}\right) - 2\frac{c}{\sigma_1}\tan\left(45 - \frac{\phi}{2}\right)}$$

Here, p_i is active earth pressure, k_{wa} is the coefficient of active radial earth pressure, q is overburden load, γ is unit weight, A refers to the horizontal area of differential soil element at z, c_w = c tan δ/tan ϕ, c is cohesion, R refers to the radius of the circular vertical shaft, r is the distance between the wall of the vertical shaft and the failure surface (released zone), δ is wall friction angle, and θ is rotated angle of major and minor principal stresses (σ_1, σ_3) at the wall. More details on the parameters can be found in Kim *et al.* (2009). As shown in Table 1, wall friction angle was assumed to be zero as did in Rankine's earth pressure theory.

To check if the earth pressure equation proposed (Kim 2011) can be appropriately applied to cohesive soil, the earth pressure on the circular vertical shaft was calculated. As shown in Table 1, all the soil properties except cohesion were assumed to be the same, simply to investigate the influence of cohesion on the earth pressure. The calculation result is shown in Fig. 1, where Fig. 1(a) represents the calculated vertical stress with depth, and Fig. 1(b) represents the earth pressure acting on the vertical shaft. The results of vertical stress and earth pressure calculated with Kim's equation (cases 12-14) were compared with that calculated with Rankine's equation (case 11).

As shown in Fig. 1, the greater the cohesion, the greater the vertical resistance, as for the arching effect. Therefore, the earth pressure acting on the vertical shaft decreased as the cohesion

Table 1 Soil properties with varying cohesion

Case	γ, kN/m³	c, kPa	ϕ, °	δ, °	k_{wa}
11	18	0	30	-	Rankine
12	18	0	30	0.0	Proposed
13	18	5	30	0.0	Proposed
14	18	10	30	0.0	Proposed

(a) Vertical stress   (b) Earth pressure
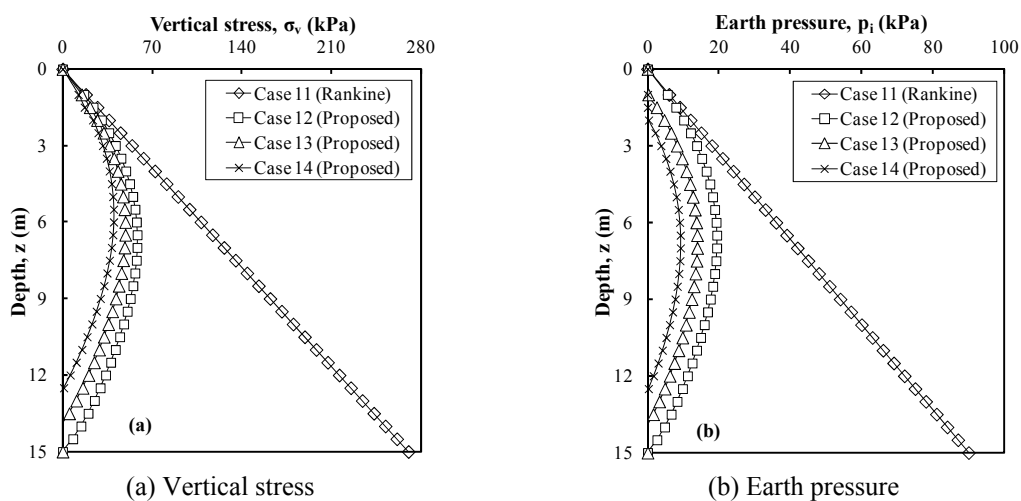
Fig. 1 Vertical stress and earth pressure according to cohesion
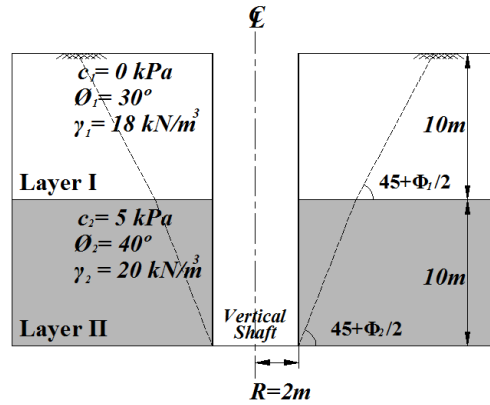
Fig. 2 Soil profile and failure surface in multi-layered ground
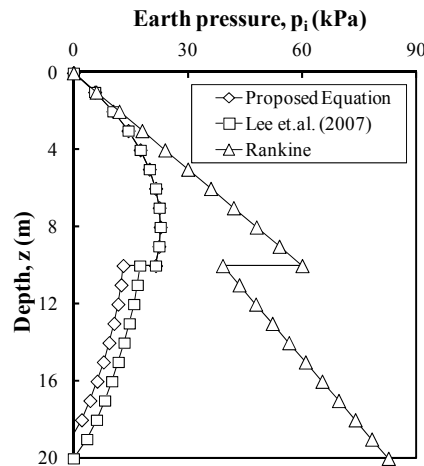
Fig. 3 Earth pressure distributions in multi-layered ground

increased. When the maximum earth pressures were compared, case 13 with 5 kPa cohesion was lower than case 12 by about 28%, while case 14 with 10 kPa was lower by about 52%. This shows that even small cohesion can considerably reduce the earth pressure. To examine whether Kim's equation (2011) can be appropriately applied to the multi-layered ground, a soil profile was assumed, as shown in Fig. 2. The layer (I) was assumed to be cohesionless soil, while the deeper layer (II) was assumed to be a c-ϕ soil. To calculate the earth pressure, the failure surface was set as shown in Fig. 2. To check the applicability of Kim's equation (2011), its result was compared with those from Lee *et al.*'s equation (2007), and Rankine's equation (1857). Fig. 3 shows the earth pressures calculated by three earth pressure equations. The Kim's equation had the same result as that of Lee *et al.*'s equation, in the cohesionless soil layer (I); however, it gave a lower earth pressure than that of Lee *et al.*'s equation, due to the increased arching effect by cohesion in the c-ϕ soil layer (II). Therefore, Kim's equation (2011) presents appropriate values according to the soil characteristics, both in the cohesionless and the c-ϕ soils, proving that it can be successfully applied to multi-layered soil.
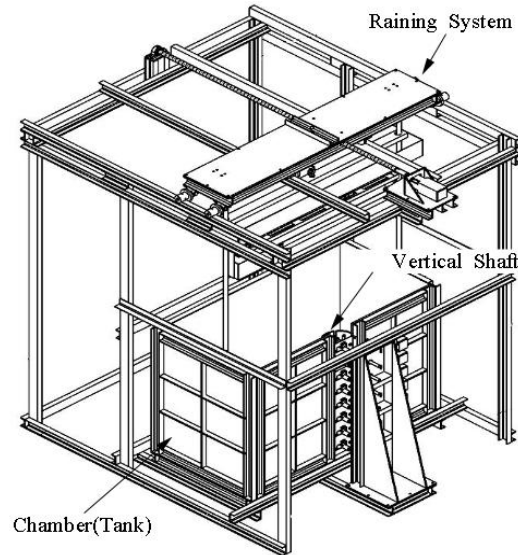
Fig. 4 Test apparatus
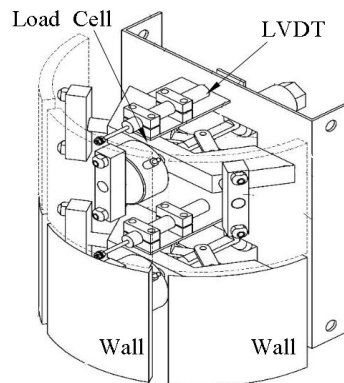
Fig. 5 Vertical shaft wall

3. Experimental test

The soil chamber was manufactured with the width of 160 cm, the length of 80 cm, and the height of 100 cm, sufficiently considering the distance to the possible failure surface as shown in Fig. 4. In the center of the front board, semi-circular walls as shown in Fig. 5 were installed to simulate the shaft walls. The total height (H) of the wall was 96 cm and the radius (R) was set at 12 cm, 14 cm, and 16 cm, which can be adjusted to correspond with the shape ratios (H/R) of 8.0, 6.857, and 6.0, respectively. To simulate the multi-step excavation and measure the earth pressure acting on the shaft wall with depth, the shaft wall was manufactured to have 8 segments with the height of 12 cm. The semi-circular wall of each segment was divided into three parts with an angle of 60° as shown in Fig. 5. The load and the displacement were measured at the middle of the three wall parts.

The soil was Jumumjin filtered sand classified as *SP* by USCS (Unified Soil Classification System). Through the sieve analysis and specific gravity tests, its effective size, D_{10} (mm), uniformity coefficient, C_u, coefficient of gradation, C_c, and specific gravity, G_s, were 0.46, 1.63, 0.91, and 2.625, respectively. The ground in the chamber was created by raining method to obtain the uniform ground. Sand was dropped from a constant height of 80 cm, then filtered out by the two dispersion sieves and distributed into the soil chamber. The unit weight and the internal friction angle were 15.2 kN/m^3 and 39.1°, respectively. Internal friction angle was obtained by direct shear tests.

To simulate the excavation method, two methods were examined; that is, the single-step excavation that bores the shaft in a lump and the multi-step excavation that bores from the top in order by using 8 separated walls (segments). The excavation was simulated by moving the shaft wall to the direction opposite to the ground that generates an active earth pressure, where the movement speed was set to 1.0 mm/min. To minimize the test error, only the earth pressure measured at the middle of the three wall parts was recorded. To simulate the *c-ϕ* soil, this study used the concept of apparent cohesion in unsaturated soil proposed by Lee *et al*. (2010). The ground in the chamber was prepared with the water content of 0.5% in order to generate the least level of cohesion to the extent that allowed the raining method.

4. Experimental test results

4.1 Earth pressure distribution at single-step excavation

Fig. 6 shows the earth pressure distribution with depth according to the wall displacement at single-step excavation, where *H/R* = 6.857. The initial earth pressure immediately after the ground was deposited was found to linearly increase with depth. The earth pressure decreased with the wall displacement; more specifically, the decrement of the earth pressure was larger with increasing wall displacement in the lower portion of the shaft than in the upper portion. Even if wall displacement was tested to reach up to 5.5 mm, the minimum active earth pressure was
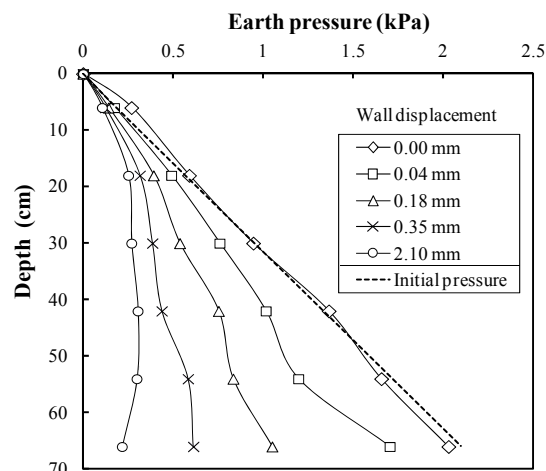
Fig. 6 Earth pressure according to wall displacement

Earth pressure, p$_i$ (kPa)
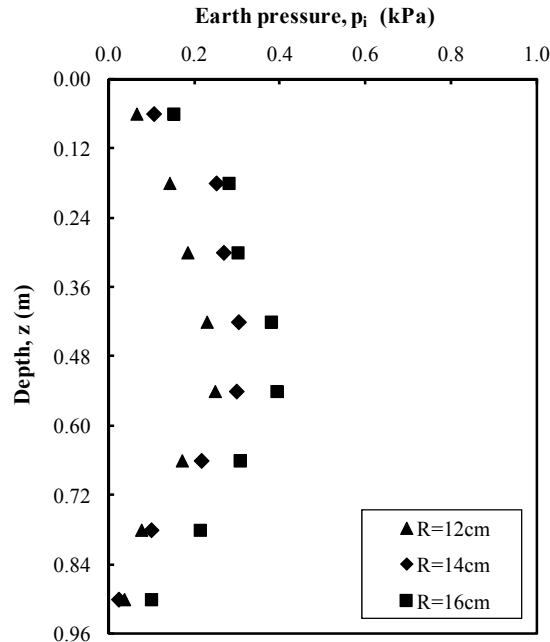
Fig. 7 Earth pressure according to wall radius

reached at 2.1 mm wall displacement. This value corresponds to 1.5% of the wall radius (*R*), which agrees with previous researches (Fujii *et al*. 1994, Herten and Pulsfort 1999, Shin 2004, Lee *et al*. 2007, Tobar and Meguid 2011), attesting to the occurrence of minimum active earth pressure around of 0.25%~6% of wall radius. At 2.1 mm wall displacement, the earth pressure of the upper and lower portions was smallest, whereas the earth pressure of the middle portion was the largest. This is because the yielding shape is conical. The decrement of earth pressure at the lower portion increases, since the volume of the active soil body per unit depth decreases with depth and shear resistance along the failure surface resists the vertical load of the active soil body, which causes the weight of the active soil body to be transferred to the stable ground.

Fig. 7 shows earth pressure with depth according to the wall radii. As the radius increases, i.e., as the *H/R* decreases, the earth pressure increases. This is because as *H/R* decreases, failure surface and released zone increase. Although shear resistance along the failure surface increases with increasing failure surface, the increment of resistance is less than that of the vertical load of the active soil body due to the increase of the released zone. The tendency of earth pressure distribution with depth was identical to that theoretically calculated, however, the measured value was relatively smaller than that theoretically calculated. This is because the earth pressure was measured at single-step excavation, which cannot take into account the earth pressure (load) recovery.

4.2 Earth pressure distribution at multi-step excavation

4.2.1 Earth pressure distribution in φ soil

Fig. 8 shows the active earth pressure with depth typically at the 8th excavation step during multi-step excavation (8 steps in total) in φ soil, where *H/R* = 8.0. Similar to single-step excavation,
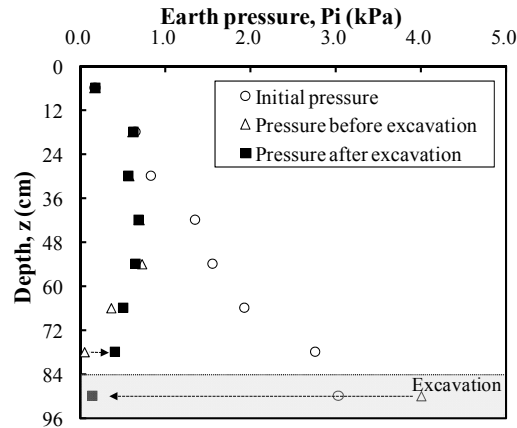
Fig. 8 Earth pressure at 8th excavation step

the earth pressure decreased from earth pressure at rest to active earth pressure. However, at multi-step excavation, the decreased earth pressure was reinstated to increase during sequential excavation of the subsequent steps. This is due to the recovery of the load which was transferred to the lower ground by the arching effect during excavation, when the subsequent excavation of the lower ground is conducted, inducing the increase of released zone and displacement. Such load recovery occurred more significantly when the subsequent excavation of the lower ground was performed; however, the recovery became insignificant from the point in which the third or lower step (below 36 cm) was excavated. It was found, with the same concept, that the load of the upper portion was transferred to the lower portion during sequential excavation, so the earth pressure immediately prior to excavation (△ in Fig. 8) was the greatest compared with the earth pressure at rest (○ in Fig. 8).

Changes in earth pressure during multi-step excavation at the depth of 6.0 cm (depth to the center of 1st wall) and 42 cm (depth to the center of 4th wall) are expressed in Fig. 9. The tendency for earth pressure to sharply decrease when each corresponding depth is excavated, and then for earth pressure to increase during the subsequent excavation steps, is similar; however, their rates of increase differ. For the 6.0 cm depth, a relatively shallow depth, the earth pressure measured prior to excavation of the corresponding 1st step is the same as the earth pressure at rest measured at the time of the preparation of ground specimen; after the excavation of the corresponding 1st step, however, the earth pressure is considerably decreased, changing from earth pressure at rest to active earth pressure, which is later fully recovered to the initial earth pressure during the subsequent lower ground excavation. For the 42 cm depth, in contrast to the 6.0 cm depth, the earth pressure measured prior to excavation of the corresponding 4th step is larger than the earth pressure at rest. Most of earth pressures exerted on 1st, 2nd and 3rd walls before excavation are transferred to 4th wall. After the excavation of the 4th step, the earth pressure is found to significantly decrease; however, it is relatively not as recovered even though sequential lower ground excavation is conducted. Nevertheless, the two cases are similar in terms of the recovery magnitude. These findings can be explained by the arching effect and load recovery. Only the typical results of 1st and 4th walls are shown in Fig. 9, since the results of other walls are same in tendency.

Fig. 10 shows active earth pressure with depth according to *H/R* for both single-step and multi-

step excavation. The final earth pressure of multi-step excavation was larger than that of single-step excavation. When comparing maximum earth pressure measured at the 4th or 5th wall, the earth pressure of multi-step excavation was 1.5~3.0 times larger than that of single-step excavation. This can be explained by the load transfer and recovery as described above. Although the value of earth pressure clearly differs, the tendencies of earth pressure are identical, which demonstrates that for the circular vertical shaft in both cases, 3-dimensional rather than 2-dimensional earth pressure is generated due to the arching effect. In multi-step excavation, the experimental result agrees well with the theoretical calculation in respect of the earth pressure distribution and earth pressure values. This could be because the earth pressure recovery (based on the arching effect) in multi-step excavation was considered.

4.2.2 Earth pressure distribution in c-ϕ soil

For the three cases of shape ratios, changes in earth pressure during multi-step excavation were measured in *c-ϕ* soil. Similar to the case of *ϕ* soil (Fig. 8), the active earth pressure with depth in each excavation step was measured and reviewed. Similar to *ϕ* soil, the earth pressure clearly

(a) Depth of 1st wall

(b) Depth of 4th wall
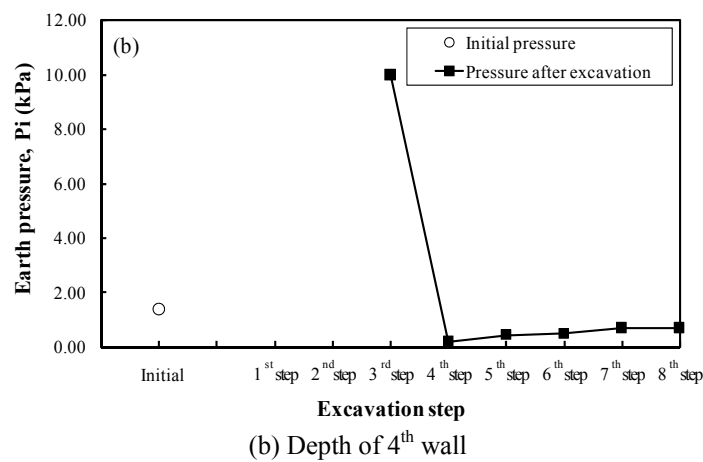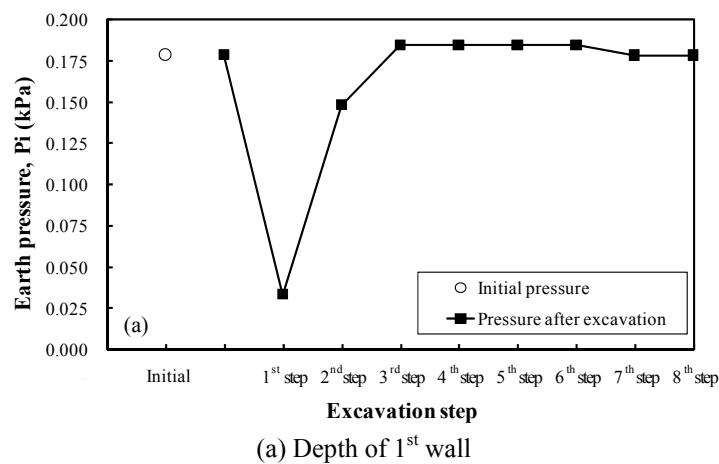
Fig. 9 Earth pressure at specific depth
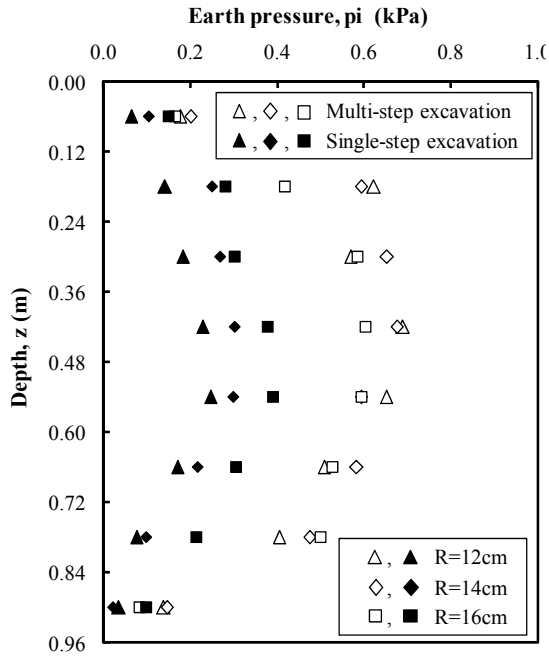
Fig. 10 Final earth pressure in ϕ soil

decreased from earth pressure at rest to active earth pressure with respect to each excavation step. The decreased earth pressure increased again due to earth pressure recovery during the sequential excavation of subsequent steps. In the case of *c-ϕ* soil, however, the recovery of earth pressure and its influential boundary were relatively small compared with ϕ soil. This is because the shear strength along the failure surface increases due to the cohesion. Like ϕ soil, the earth pressure immediately prior to the excavation of the pertinent step was greatest compared with the earth pressure at rest. However, the increment of earth pressure shown just before the excavation was
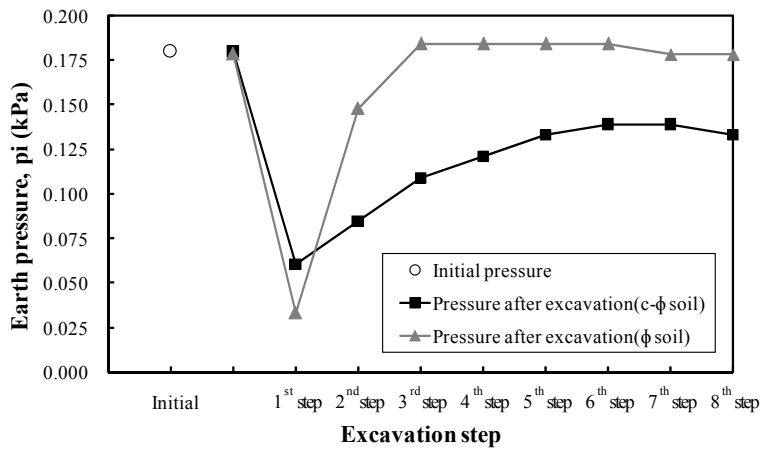
Fig. 11 Earth pressure at depth of 6.0cm (1st wall)

relatively small compared with φ soil. Changes in earth pressure during multi-step excavation at the depth of 6.0 cm are presented in Fig. 11. Changes in earth pressure in *c-φ* soil showed a similar trend to the case of *φ* soil. During the sequential excavation by step, the earth pressure, as for the upper steps (shallow depth), was recovered almost to the initial earth pressure compared with that for the lower steps (deep depth); however, the amount of load recovery was relatively small as a whole due to cohesion compared with *φ* soil, consequently resulting in a smaller final earth pressure.

Fig. 12 shows active earth pressure with depth according to *H/R* for both *φ* soil and *c-φ* soil. For both soils, earth pressure was smallest at the upper and lower portions and largest at the middle portion. As shown in Fig. 12, even a small amount of cohesion can cause a significant decrease in earth pressure. This is because cohesion allows shear resistance to increase, reduces the released zone, and consequently reduces load recovery over all. Earth pressure did not change significantly according to *H/R* in both ground conditions. Resulting from the direct shear test performed to measure the cohesion of the *c-φ* soil used, the *c-φ* soil was found to have the same internal friction angle as that of *φ* soil, with a slight level of cohesion, although its value was not easily measurable. In order to infer apparent cohesion mobilized in *c-φ* soil, the test results (Fig. 12) in *c-φ* soil were compared with the results theoretically calculated. As a result, the laboratory test result and the theoretically calculated result were the most consistent when apparent cohesion was 0.4 kPa. This finding indicates that even a lower cohesion of 0.4 kPa can contribute to decrease the earth pressure by about 35%~45%.

4.2.3 Earth pressure distribution in multi-layered ground

To investigate the changes in earth pressure in a multi-layered ground during multi-step
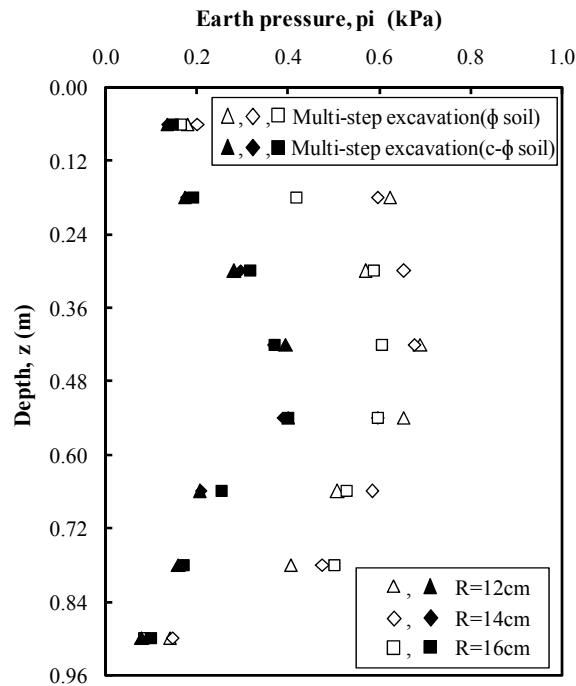
Fig. 12 Earth pressures for both *φ* soil and *c-φ* soil
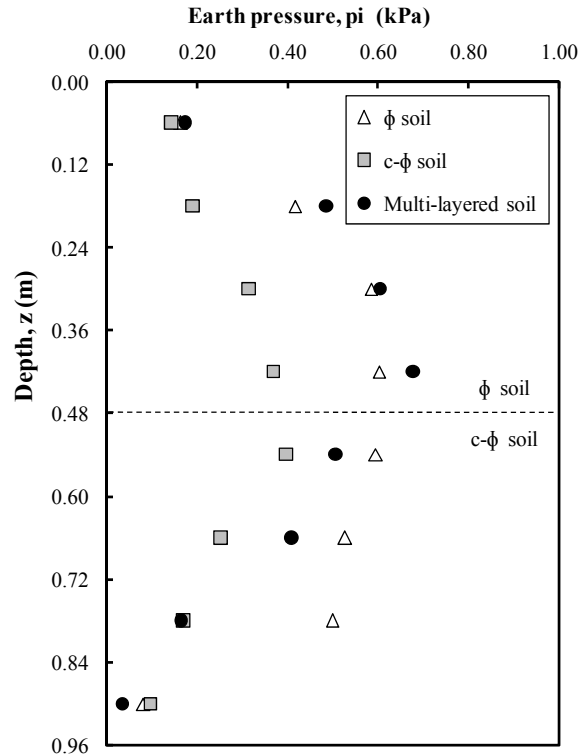
Fig. 13 Earth pressure in multi-layered ground

excavation, a ground was prepared consisting of the upper half (48 cm depth from 1st to 4th walls) filled with dry sand (ϕ soil), and the lower half (48 cm depth from 5th to 8th walls) filled with unsaturated sand with 0.5% water content (c-ϕ soil). The shaft wall was set to be $H/R = 6.0$. The test results in the multi-layered ground showed a similar trend in earth pressure distribution to other cases (single-layered ϕ or c-ϕ soil). The earth pressure decreased from earth pressure at rest to active earth pressure and then increased again with the sequential excavation.

The changes in earth pressure in the multi-layered ground during multi-step excavation are shown in Fig. 13 together with the results in the ϕ soil and c-ϕ soil. The earth pressures of the 4th and 5th walls that demarcated the soil condition into the upper ϕ soil and the lower c-ϕ soil showed significant difference. This is due to the difference in shear resistance according to the ground condition. Apparent cohesion exists in the lower ground, so shear resistance is relatively larger than that in the upper ground. In upper ground, the earth pressure in multi-layered ground was almost similar to that in single-layered ϕ soil, whereas in lower ground, the earth pressure in multi-layered ground was found to be smaller than that in single-layered ϕ soil, although larger than that in single-layered c-ϕ soil. This is due to the fact that since shear resistance along the failure surface of the upper ϕ soil is smaller compared with a single-layered c-ϕ soil, the larger vertical load subjected to the lower c-ϕ soil is induced and consequently the larger earth pressure is found in the lower c-ϕ soil compared with single-layered c-ϕ soil; meanwhile, the earth pressure in the lower c-ϕ soil becomes smaller compared with that in the single-layered ϕ soil due to the increase of shear resistance of the lower c-ϕ soil.

5. Verification of new earth pressure equation

5.1 Comparison with experimental test results

To verify the new earth pressure equation proposed (Kim 2011), the earth pressure estimated by using the proposed equation is compared with the experimental test results. Fig. 14 shows test results for both single-step excavation and multi-step excavation under the condition of $H/R = 6.0$ and ϕ soil. It also shows earth pressure distributions calculated by using the new earth pressure equation (Kim 2011) as well as those estimated by using other theoretical equations proposed in the previous studies. It was found that the earth pressures proposed by Berezantzev (1958) and Shin (2004) (who both assumed a value of λ, the coefficient of tangential earth pressure is equal to 1.0), are smaller than those proposed by Prater (1977) and Kim (2011), both of which assumed a value of $\lambda = 1.0 - \sin \phi$. The earth pressures predicted by Berezantzev (1958) and Shin (2004) were similar to those of the test result of single-step excavation, while the earth pressure predicted by Kim (2011) was similar to that of the test result of multi-step excavation and the earth pressure predicted by Prater (1977) was overestimated. Considering that the shaft on a real site is constructed step by step (multi-step excavation), it can be concluded that the earth pressure predicted by Kim (2011) is fittest to the case of ϕ soil.

Fig. 15 shows the test results in *c-ϕ* soil as well as earth pressures estimated by the various theoretical equations. When the cohesion of 0.4 kPa was applied, Berezantzev (1958) predicted negative earth pressure, while Kim (2011) predicted 0.0 in the uppermost ground and negative value in the lowermost ground. Although Shin's equation (2004) predicts similar values as those of the test results, it cannot consider cohesion, therefore making it difficult to apply to *c-ϕ* soil. The
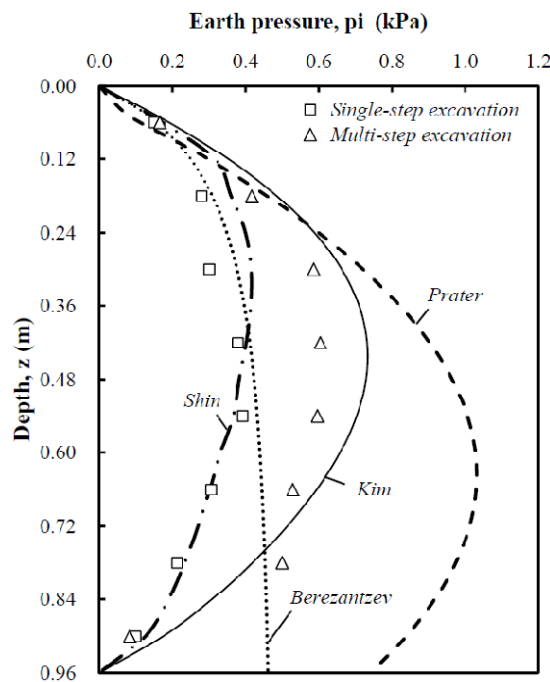
Fig. 14 Comparison with theoretical equations in ϕ soil
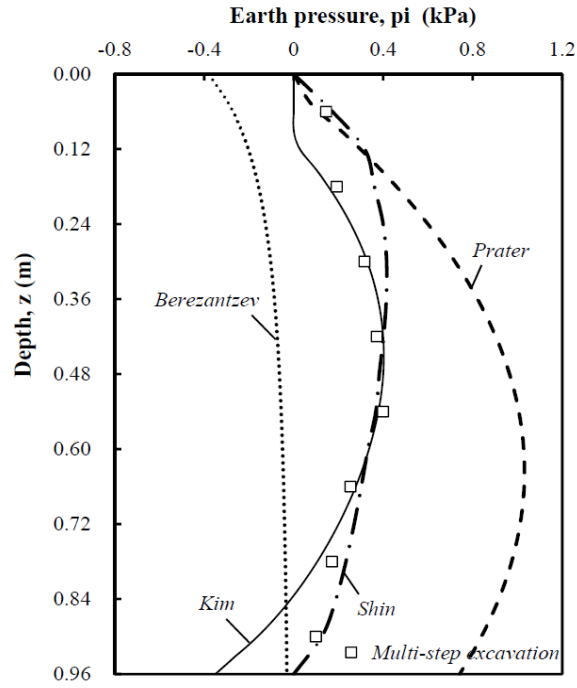
Fig. 15 Comparison with theoretical equations in *c-φ* soil
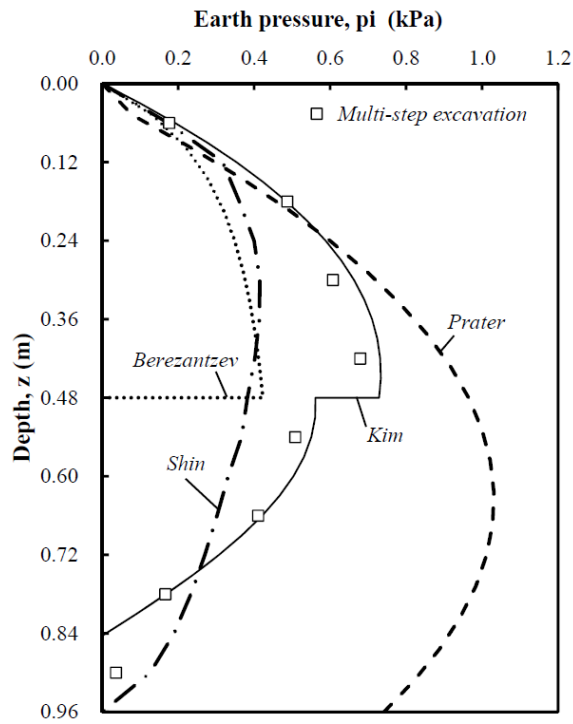
Fig. 16 Comparison with theoretical equations in multi-layered soil

equation of Berezantzev (1958) is considered to not predict earth pressure appropriately because it cannot produce the arch shaped earth pressure distribution shown in the test result. Accordingly, it is considered that the equation of Kim (2011) can predict earth pressure relatively well in the *c-ϕ* soil, although it yields slight difference to that of the test result.

Fig. 16 shows both test results and earth pressures estimated by theoretical equations in multi-layered ground. While the equations of Berezantzev (1958) and Kim (2011) that can consider cohesion clearly reflect changes in earth pressure according to the ground condition, Prater's (1977) and Shin's (2004) equations that cannot consider cohesion show the same tendency of earth pressure distribution irrespective of the ground condition. Shin (2004) underestimated the earth pressure generally, whereas Prater (1977) overestimated. Similar to single-layered *c-ϕ* soil, Berezantzev (1958) predicted negative earth pressure in the lower ground having cohesion. The equation of Kim (2011) is found to predict earth pressure appropriately even for the multi-layered ground since it considers shear resistance according to the characteristics of *ϕ* soil and *c-ϕ* soil.

5.2 Comparison with field measurement data

To verify the coefficient and equation of radial earth pressure proposed (Kim 2011), the earth pressure estimated by using the proposed equation is compared with the actual field measurement data, as well as those estimated by using other earth pressure equations. The circular vertical shaft for the field measurement was constructed with a diameter of 6 m and depth of 14 m. The ground was composed of reclaimed soil, weathered soil, and weathered rock, in order from the ground

Table 2 Soil properties of construction site

Soil type	γ, kN/m^3	c, kPa	ϕ, °	E, MPa	Depth, m
Reclaimed soil	17.9	0.0	21.0	10.7	0~6.2
Weathered soil	19.5	10.5	25.3	23.2	6.2~12.0
Weathered rock	20.6	30.0	31.8	33.8	12.0~14.0
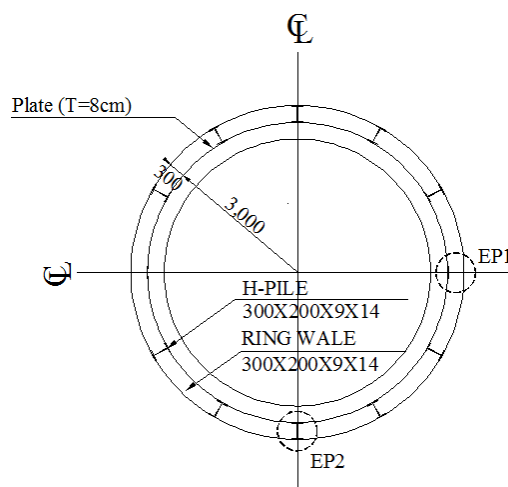
Fig. 17 Cross section of vertical shaft

surface. The temporary earth retaining structure was installed with plates, H-piles, and ring-wales. Fig. 17 shows the cross section of the constructed shaft. The soil properties are presented in Table 2. *E* in Table 2 refers to the elastic modulus. The excavation was carried out step by step (multi-step excavation), and five ring-wales were installed at 3 m intervals. The earth pressure was measured at EP1 and EP2, as shown in Fig. 17, with earth pressure cells of vibration wire type. Ten earth pressure cells were installed at 1.5 m intervals, from 1 m below the ground surface.

Fig. 18 shows the earth pressures calculated using the theoretical equations, along with the actual field measurement data (average value of EP1 and EP2). As the equipment of about 20 kPa for the construction was laid on top of the ground, it was applied as the surcharge load. As the equation proposed by Prater (1977) cannot consider the surcharge load, it shows 0.0 of pressure on the ground surface. The earth pressures obtained from all equations sharply varied at the depths of 6.2 m and 12.0 m, where the soil properties changed. The field measurement value also showed a difference in earth pressure at the depth of 6.2 m, where the layer changes. Berezantzev's equation (1958) and the proposed new equation, which can consider the cohesion, produced smaller earth pressures in the reclaimed soil and weathered soil than Prater's (1977) and Wong and Kaiser's (1988) equations, neither of which can consider the cohesion, and showed 0.0 of earth pressure in weathered rock having 30 kPa of cohesion. In the field measurement data, the earth pressure increased with depth in the reclaimed soil layer, decreased in the weathered soil layer due to the cohesion, and became 0.0 in the weathered rock layer. These field measurement values were most similar with the earth pressure predicted by the proposed equation (Kim 2011). Therefore, the earth pressure equation proposed (Kim 2011) can be considered as the most appropriate equation, because it can consider the surcharge load and the arching effect, according to the soil properties.
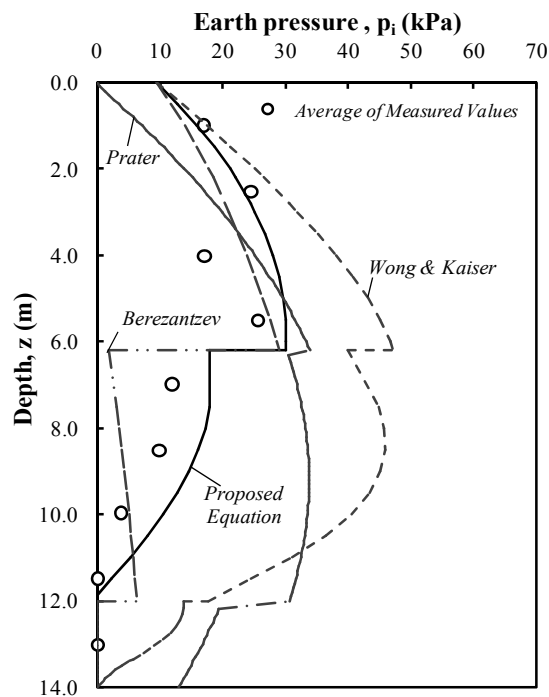
Fig. 18 Comparison of field data with theoretical equations

6. Conclusions

A new earth pressure equation considering the arching effect in c-ϕ soils was proposed for the accurate calculation of earth pressure on circular vertical shafts. The arching effect and the subsequent load recovery phenomenon occurring due to multi-step excavation were quantitatively investigated through laboratory tests. The new earth pressure equation was verified by comparing the test results with the earth pressures predicted by new equation in various soil conditions. The conclusions from the study are as follows:

(1) To examine the appropriateness of the proposed earth pressure equation, its result was compared with those of other existing equations. The results showed that the proposed earth pressure equation appropriately considers the decrease of vertical stress due to the cohesion, proving its unique applicability in c-ϕ soils.

(2) The test results showed that the earth pressure was measured in an arch shape where earth pressure was largest in the middle portion yet smallest in the upper and lower portions due to the arching effect of backfill. The wall displacement needed for the minimum active earth pressure was found to be approximately 1.5% of the wall radius, which is consistent with the range of previous studies.

(3) From testing using multi-step excavation in ϕ soil, the arching effect was clearly observed, showing that the earth pressure that had been decreased by load transfer was reinstated due to the load recovery during sequential excavation of subsequent steps. If excavation for the shaft is made from the top to the bottom step by step (multi-step excavation), the load recovery induces earth pressure larger than in the case of single-step excavation.

(4) The test performed in c-ϕ soil resulted in the occurrence of the arching effect similarly to that in ϕ soil, while earth pressure greatly decreased even with the small amount of cohesion. Therefore, predicting earth pressure without considering such cohesion can lead to overestimation of earth pressure.

(5) From testing in various ground conditions, it was found that the newly proposed equation, which enables consideration of cohesion as appropriate, is the most reliable equation for predicting earth pressure in both ϕ soil and c-ϕ soil. The comparison of the theoretical equations with the field data measured on a real construction site also highlighted the best-fitness of the theoretical equation proposed by Kim (2011) in predicting earth pressure.

Acknowledgments

References

Berezantzev, V.G. (1958), "Earth pressure on the cylindrical retaining walls", *Proceedings of International Society of Soil Mechanics and Foundation Engineering* (*ISSMFE*) *Conference on Earth Pressure Problems*, Butterworths, London, UK, September, pp. 21-27.

Cheng, Y.M., Hu, Y.Y. and Wei, W.B. (2007), "General axisymmetric active earth pressure by method of characteristics – theory and numerical formulation", *Int. J. Geomech.*, **7**(1), 1-15.

Fujii, T., Hagiwara, T., Ueno, K. and Taguchi, A. (1994), "Experiment and analysis of earth pressure on an axisymmetric shaft in sand", *Proceedings of the 1994 International Conference on Centrifuge*, Singapore, August, pp. 791-796.

Herten, M. and Pulsfort, M. (1999), "Determination of spatial earth pressure on circular shaft constructions", *Granular Matter*, **2**(1), 1-7.

Imamura, S., Nomoto, T., Fujii, T. and Hagiwara, T. (1999), "Earth pressures acting on a deep shaft and the movements of adjacent ground in sand", *Proceedings of the International Symposium on Geotechnical Aspects of Underground Construction in Soft Ground*, Tokyo, Japan, July, pp. 647-652.

Iskander, M., Chen, Z., Omidvar, M., Guzman, I. and Elsherif, O. (2013), "Active static and seismic earth pressure for c-φ soils", *Soils Found.*, **53**(5), 639-652.

Ismeik, M. and Shaqour, F. (2015), "Seismic lateral earth pressure analysis of retaining walls", *Geomech. Eng., Int. J.*, **8**(4), 523-540.

Kim, D.H. (2011), "Characteristics of lateral earth pressure acting on a circular vertical shaft", Ph.D. Dissertation; Korea University, Seoul, Korea.

Kim, D.H., Lee, D.S., Kim, K.R., Lee, Y.H. and Lee, I.M. (2009), "Earth pressures acting on vertical circular shafts considering arching effects in c- φ soils: I. Theory", *Tunn. Technol.*, **11**(2), 117-129.

Lee, I.M., Moon, H.P., Lee, D.S., Kim, K.R. and Choi, M.S. (2007), "Earth pressure of vertical shaft considering arching effect in layered soils", *Tunn. Technol.*, **9**(1), 49-62.

Lee, I.M., Jung, J.H., Kim, K.R. and Kim, D.H. (2010), "Effect of apparent cohesion in unsaturated soils on the ground behavior during underground excavation", *Tunn. Technol.*, **12**(2), 117-127.

Liu, F.Q. and Wang, J.H. (2008), "A generalized slip line solution to the active earth pressure on circular retaining walls", *Comput. Geotech.*, **35**(2), 155-164.

Liu, F.Q., Wang, J.H. and Zhang, L.L. (2009), "Axi-symmetric active earth pressure obtained by the slip line method with a general tangential stress coefficient", *Comput. Geotech.*, **36**(1-2), 352-358

Moradi, G. and Abbasnejad, A. (2015), "Experimental and numerical investigation of arching effect in sand using modified Mohr Coulomb", *Geomech. Eng., Int. J.*, **8**(6), 829-844.

Nian, T.K., Liu, B., Han, J. and Huang, R.Q. (2014), "Effect of seismic acceleration directions on dynamic earth pressures in retaining structures", *Geomech. Eng., Int. J0*, **7**(3), 263-277.

Prater, E.G. (1977), "An examination of some theories of earth pressure on shaft linings", *Can. Geotech. J.*, **14**(1), 91-106.

Rankine, W.J.M. (1857), "On the stability of Loose Earth", *Phil. Trans. Royal Society*, **147**(1), 9-27.

Shin, Y.W. (2004), "Earth pressure acting on the cylindrical retaining wall of a shaft in cohesionless soils", Ph.D. Dissertation; Hanyang University, Seoul, Korea.

Shukla, S.K., Gupta, S.K. and Sivakugan, N. (2009), "Active earth pressure on retaining wall for c-φ soil backfill under seismic loading condition", *J. Geotech. Geoenviron. Eng.*, **135**(5), 690-696.

Terzaghi, K. (1943), *Theoretical Soil Mechanics*, John Wiley and Sons, Hoboken, NJ, USA.

Tobar, T. and Meguid, M.A. (2010), "Comparative evaluation of methods to determine the earth pressure distribution on cylindrical shafts: A review", *Tunn. Undergr. Space Technol.*, **25**(2), 188-197.

Tobar, T. and Meguid, M.A. (2011), "Experimental study of the earth pressure distribution on cylindrical shafts", *J. Geotech. Geoenviron. Eng.*, **137**(11), 1121-1125.

Wong, R.C.K. and Kaiser, P.K. (1988), "Design and performance evaluation of vertical shafts; rational shaft design method and verification of design method", *Can. Geotech. J.*, **25**(2), 320-337.

Zheng, D.F., Nian, T.K., Liu, B., Yin, P. and Song, L. (2015), "Coefficient charts for active earth pressures under combined loadings", *Geomech. Eng., Int. J.*, **8**(3), 461-476.

GC